

# Pairing symmetry in iron-based superconductors

Caizhi Xu  
Department of Physics  
University of Illinois Urbana-Champaign

**Abstract:** Iron-based superconductor is a new type of unconventional superconductors. It is similar to cuprates in some ways, but they have many significant differences. The antiferromagnetic spin fluctuations seem to play a very important role in the pairing mechanism. This paper will briefly talk about the theories and experimental findings on the pairing mechanism of this new type of superconductors.

# 1. Introduction

Superconductivity has always been an important topic in Physics. In 1911, Heike Kamerlingh Onnes and co-workers found that the electrical resistivity of mercury (Hg) abruptly dropped to zero when it was cooled below 4.2K<sup>1</sup>. Since then, superconductivity attracted lots of scientists to study. One reason is that it can bring huge economical benefits. If we can achieve room-temperature superconductivity, the energy lost on resistive wires can be saved. Another important reason is that there are many puzzles in this field, which remain to be solved.

In 1957, Bardeen, Cooper and Schrieffer put up with the famous BCS theory<sup>2</sup>. At that time it is very successful in explaining many phenomena. In 1986, Bednorz and Müller discovered the high-temperature superconductivity<sup>3</sup>, which cannot be explained by the BCS theory. In a short time, scientists all over the world discovered more high-temperature superconductors, and they are called cuprates. Though lots of study has been done, puzzles remain.

In 2008, Kamihara et al. discovered a new type of high-temperature superconductor, LaFeAsO doped with Fe on the oxygen site ( $T_c=26K$ )<sup>4</sup>. Later on, some other high-temperature superconductors which contain Fe were found. They are called iron-based superconductors. To date, the highest  $T_c$  in this class of material has been raised to 55K<sup>5</sup>.

Compared to Cuprates, iron-based superconductors have some similarities. Firstly, both of their parent compounds are anti-ferromagnets. Increased doping can destroy anti-ferromagnetism and lead to superconductivity. Secondly, superconductivity occurs in specific planes. In cuprates, it is Cu-O plane. While in iron-based superconductors, it is Fe-As plane. However, deeper studies show that they also have significant differences. For Cuprates, its parent compound is a special type of antiferromagnet—a Mott insulator; While in iron-based superconductors, it is an anti-ferromagnetic “spin-density-wave” metal. Moreover, the  $Cu_{3-x}Fe_xO_{2-y}$  contributes to superconductivity; while in iron-based superconductors, all five Fe3d orbitals contribute to superconductivity<sup>6</sup>. These differences make this new type of high-temperature superconductors very interesting.

In this paper, first I will briefly talk about theoretical backgrounds of superconductivity. Then I will introduce some experimental findings of iron-based superconductors (FeSCs). Some theorists claim that the pairing symmetry of FeSCs is  $S_{\pm}$ . Some experiments which support this claim will be in the latter part of this paper.

However, the  $S_{\pm}$  pairing may not be true in FeSCs. There are some controversies, which will also be discussed.

## 2. Theoretical backgrounds

### 2.1 ODLRO (Off-Diagonal Long Range Order)<sup>7</sup>

ODLRO is an essential condition of macroscopic phenomena such as superconductivity<sup>8</sup>. We can express it as a nonzero expectation value of the two-particle reduced density matrix:

$$\rho_2(r, r') = \langle \Psi_\alpha^\dagger(r) \Psi_\beta^\dagger(r) \Psi_\alpha(r') \Psi_\beta(r') \rangle$$

Here  $\Psi_\alpha^\dagger(r)$  and  $\Psi_\alpha(r)$  are particle field operators for creating and annihilating a particle at a relative coordinate  $r$  with spin (pseudo-) state  $K \uparrow$ . For spin singlet pairing,  $\alpha = -\beta$ . In the limit of  $|r - r'| \rightarrow \infty$ , the ODLRO can be expressed as

$$\rho_2(r, r') = \langle \Psi_\downarrow^\dagger(r) \Psi_\uparrow^\dagger(r) \rangle \langle \Psi_\downarrow(r') \Psi_\uparrow(r') \rangle$$

The ODLRO in superconductors corresponds to the expectation value of local pair amplitude  $\langle \Psi_\downarrow^\dagger(r) \Psi_\uparrow^\dagger(r) \rangle$ , which is consistent with the order parameter in Ginzberg-Landau equation. In momentum space, ODLRO corresponds to  $\langle c_{k\uparrow} c_{-k\downarrow} \rangle$ . We have  $\langle c_{k\uparrow} c_{-k\downarrow} \rangle \propto \Psi(k) \propto \Delta(k)$ . ODLRO is a general property of all superconductors. Thus we can use  $\langle c_{k\uparrow} c_{-k\downarrow} \rangle \propto \Psi(k) \propto \Delta(k)$  to study the superconducting state. The gap function describes the pairing state in superconductors.

$$\Delta(k) \begin{cases} = 0 & T > T_c \\ \neq 0 & T < T_c \end{cases}$$

The gap function  $\Delta(k)$  can be measured experimentally.

### 2.2 Pairing mechanism

It is well-known that in conventional superconductors the electron-phonon interaction gives rise to the attraction between two electrons, thus forming Cooper pairs<sup>2</sup>.

In cuprates and FeSCs, the popular opinion is that the electron-phonon is not strong enough to overcome Coulomb repulsion and form Cooper pairs. Many people think that it is electron-electron coupling that leads to the formation of Cooper pairs.

### 2.3 Pairing symmetry

Since electrons are Fermions, the total wavefunction of Cooper pairs must be anti-symmetric under the exchange of coordinates. For spin-singlet (S=0), its spin wave-function is anti-symmetric. Thus its orbital wave-function must be symmetric, like s wave, d wave, g wave and so on; For spin-triplet (S=1), its spin wave-function

is symmetric. Thus its orbital wave-function must be anti-symmetric, like p wave, f wave and so on.

The Angle-resolved Photoemission Spectroscopy (ARPES) Superconducting Quantum Interference Device (SQUID) unambiguously prove that the order parameter of cuprates has  $d_{x^2-y^2}$  symmetry.

### 3. Experiments and theories on iron-based superconductors

#### 3.1 Crystal structure and Magnetism

The newly discovered iron-based superconductors have many family members. Some of the stoichiometric parent compounds include LaFeAsO (abbreviated as 1111 for its 1:1:1:1 ratio of the four elements), BaFe<sub>2</sub>As<sub>2</sub> (the 122 compounds), FeTe (the 11 compounds), LiFeAs (the 111 compounds), and the Sr<sub>2</sub>VO<sub>3</sub>FeAs (the 21311 compounds). Besides these materials, the defect structure A<sub>x</sub>Fe<sub>2-y</sub>Se<sub>2</sub> (where A=K, Rb, Cs, Tl) is also a member of this big family<sup>9</sup>.

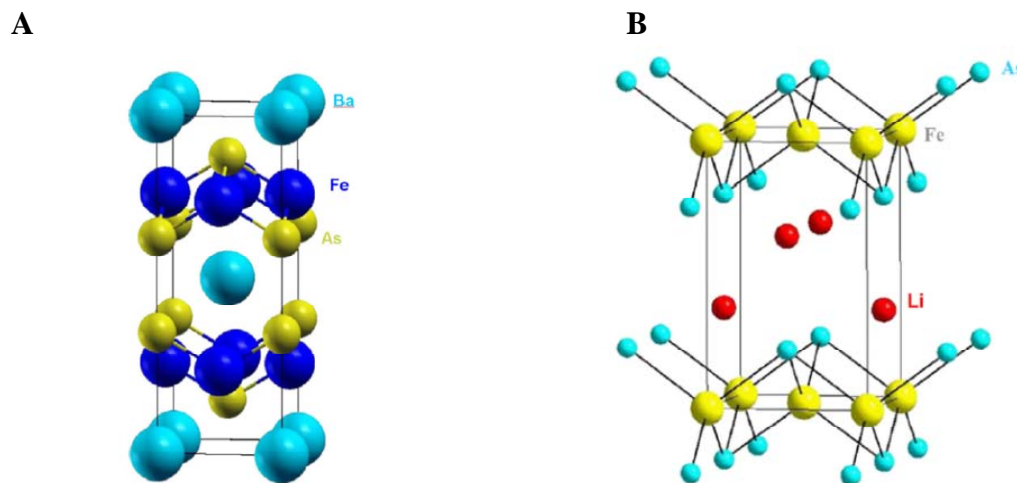


**Fig. 1.** Lattice structure of two types of iron-based superconductors. (A) 122 BaFe<sub>2</sub>As<sub>2</sub><sup>10</sup>; (B) 111 LiFeAs<sup>11</sup>.

In these materials, the superconductivity occurs in the FeX atom plane, where X=As, P, S, Se, or Te. Structurally, FeX forms a tri-layer consisting of a square array of Fe sandwiched between two checkerboard layers of X (Fig. 2A, inset). It is widely believed that superconductivity in this family originates from the electrons of the 5 3d orbitals of Fe in the FeX trilayers.

Similar to the parent compounds of Cuprates, most of the stoichiometric parent compounds of iron-based superconductors exhibit antiferromagnetism at ambient pressure. Except FeTe, the spatial arrangement of the magnetic moments in a FeX

trilayer is represented by the red arrows in Fig. 2B. Along the crystalline  $c$  axis (see Fig. 2A for the definition of  $a$ ,  $b$ , and  $c$  axes), the nearest-neighbor magnetic moments can be either parallel or anti-parallel<sup>12</sup>.

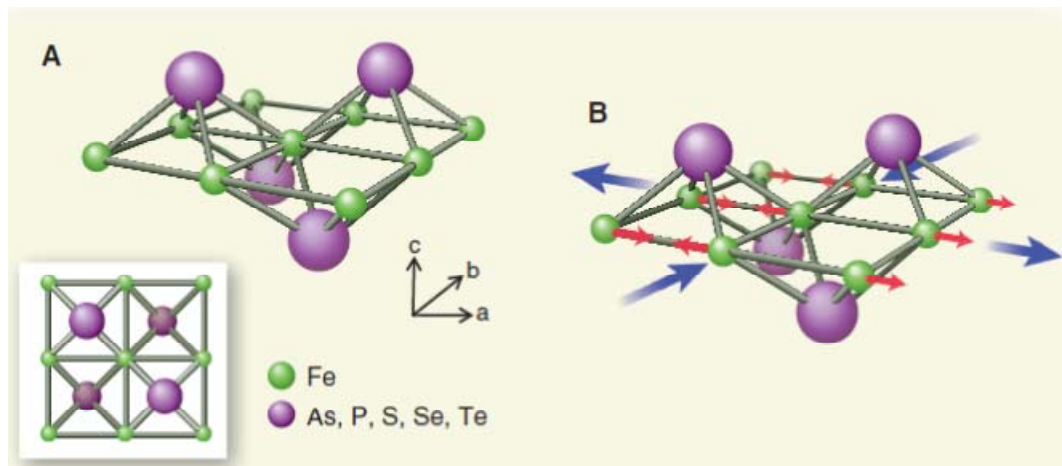


**Fig. 2.** (A) Structural motif of the FeSC. (Inset) Top view of the FeX trilayer. The triad ( $a$ ,  $b$ , and  $c$ ) demonstrates the three crystallographic directions. (B) The antiferromagnetic order of the stoichiometric iron-based materials. The red arrows represent the magnetic moments, and the blue arrows indicate the directions of structural distortion<sup>12</sup>.

### 3.3 Pairing theories

The Local Density Approximation calculation (LDA) done on the FeSCs showed that these materials have many bands and several disconnected Fermi Surfaces. For 1111 compounds, these Fermi Surfaces look like disconnected cylinders<sup>13</sup> (Fig.3A).

According to a generalization of BCS theory<sup>14</sup>, the superconductivity is possible even when the intra- and inter-Fermi Surface scatterings are both repulsive, as long as the latter dominates. Under that condition, the order parameter will have an opposite sign on the two Fermi Surfaces<sup>12</sup>(Fig.3B).

Calculations of magnetic susceptibility<sup>15</sup> gave us more insight into this class of material. It showed that FeSCs have a tendency to order antiferromagnetically. The wave vector associated with the spatial periodicity of the magnetic moments coincide with those connecting the centers of the electron and hole Fermi Surfaces in Fig.3A.

Under these observations, Mazin *et al.* put up with an idea that Antiferromagnetic spin fluctuations can induce the  $S_{\pm}$  pairing<sup>15</sup>. “S” means that the order parameter remains unchanged by the symmetry operations of the crystal, and “ $\pm$ ” means that the sign of the order parameter on electron pocket is different from that on hole pocket. Several theories based on the above itinerant electron point of view supports this idea (Fig.3C). According to them,  $S_{\pm}$  pairing is favored when the antiferromagnetism is suppressed. In addition, the most important virtual excitations that trigger the  $S_{\pm}$  pairing are the “antiferromagnetic spin fluctuations”<sup>12</sup>.

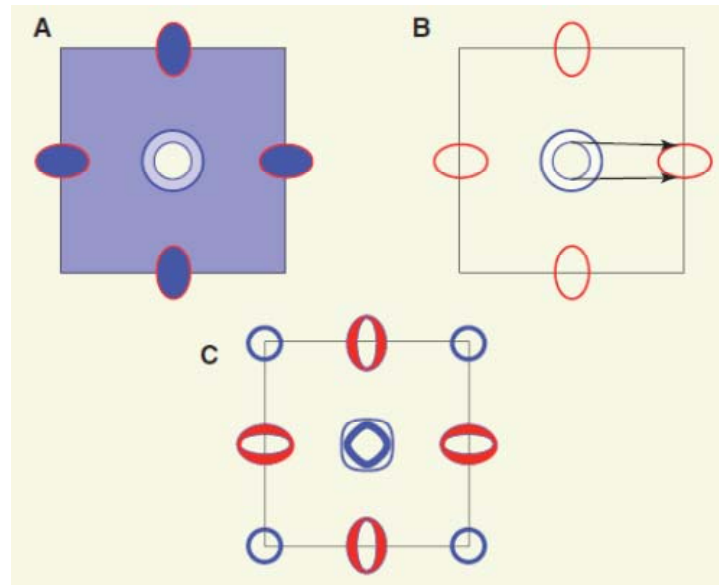


**Fig.3.** (A) Electron- and holelike FSs of FeX trilayers are indicated by the red and blue curved lines, respectively. The color shading reflects the electron occupation at each momentum point (increasing from white to blue). (B) Inter-FS pair scattering. (C) Schematic representation of the superconducting order parameter obtained from several weak coupling theories. The width of the blue and red bands represents the magnitude of the order parameter. The color represents the sign: blue, positive; red, negative. The order parameter associated with four extra-small holelike FSs at the corner of the Brillouin zone is also shown here. These extra hole FSs are present in materials with large hole doping<sup>12</sup>.

### 3.4 Experiments on pairing symmetry

#### 3.4.1 Angle-resolved photoemission spectroscopy (ARPES) and Inelastic neutron scattering.

ARPES is a powerful technique for measuring materials' electronic states. The basic principle is the simple Photoelectric Effect. As shown in Fig 4A, photons impinge on the material. The electrons inside the material will be excited, and some of them have large enough energy to come out. Then they will be collected by an analyzer. In the analyzer there is a detector which can record their momentum and energy. With the condition of energy conservation and momentum conservation along the sample surface, we can calculate the electrons' momentum and binding energy inside the material, i.e. the band structure.

Fig 4B shows a study on the temperature dependence of superconducting gap. The dashed line represents the Fermi level. As the temperature goes down, the material becomes superconducting. We can clearly see the energy gap. ARPES is a powerful tool to study the superconducting gap.

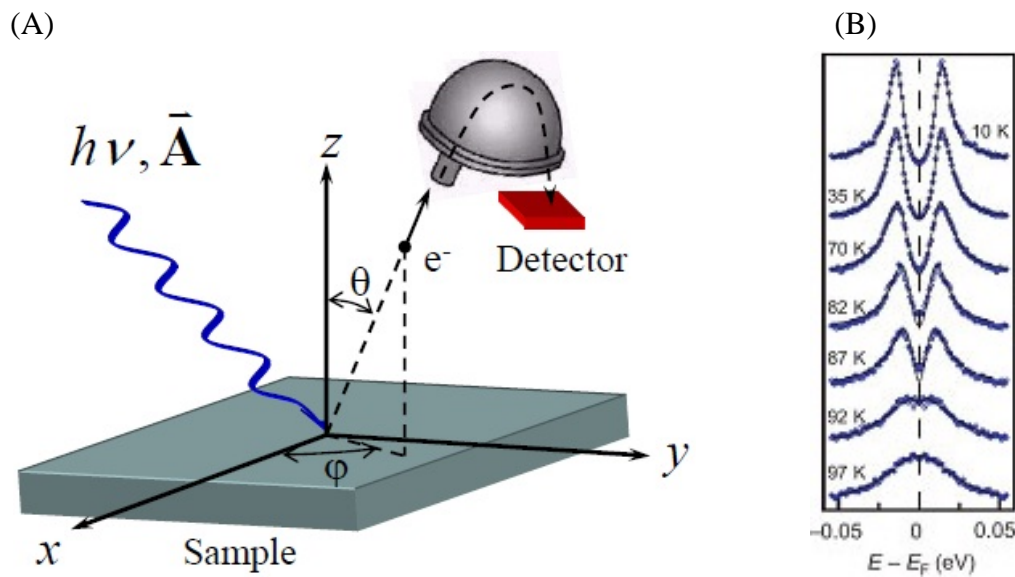


**Fig.4.** (A) Schematic diagram of ARPES (B) Temperature dependence of superconducting gap of under-doped Bi2212<sup>16</sup>

Inelastic neutron scattering is an experimental technique commonly used to study atomic and molecular motion. It can also be used to study magnetic excitation. We denote the scattering vector  $q$  as the difference between incoming and outgoing wave vector, and  $E$  as the energy change experienced by the sample (negative that of the scattered neutron). The experiment process is shown in Fig 5.  $S(q, E)$  represents the counts of neutrons with scattering vector  $q$  and energy exchange  $E$ , and is called the *dynamic structure factor*.

The electromagnetic interaction of the neutron's magnetic moment with the sample's internal magnetic fields gives rise to magnetic scattering.

Previous studies show that<sup>17</sup>, below the superconducting transition temperature, the  $S(q, E)$  is predicted to be enhanced at certain values of  $Q$  by a coherence factor, provided that the energy gap  $\Delta$  has the form  $\Delta_{k+Q} = -\Delta_k$  (here  $k$  and  $k+Q$  are wave-vectors on different parts of the Fermi surface).

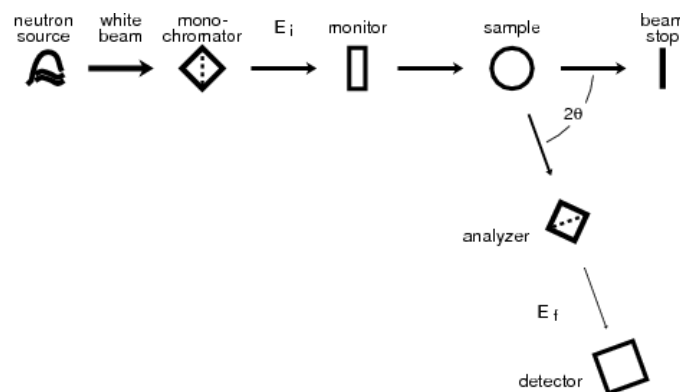


**Fig.5.** Schematic diagram of inelastic neutron scattering<sup>18</sup>

### 3.4.2 Experimental results of $\text{Ba}_{0.6}\text{K}_{0.4}\text{Fe}_2\text{As}_2$

There are many types of FeSCs. In the following I will focus on  $\text{Ba}_{0.6}\text{K}_{0.4}\text{Fe}_2\text{As}_2$ , the optimally doped material ( $T_c=38\text{K}$ ) in 122 class.

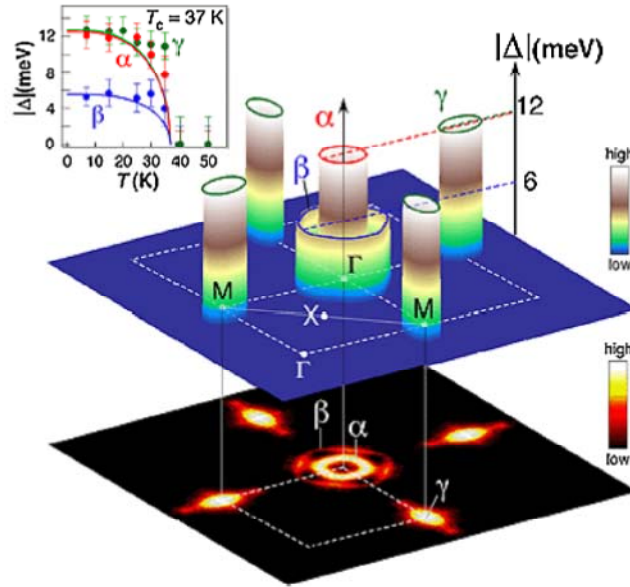
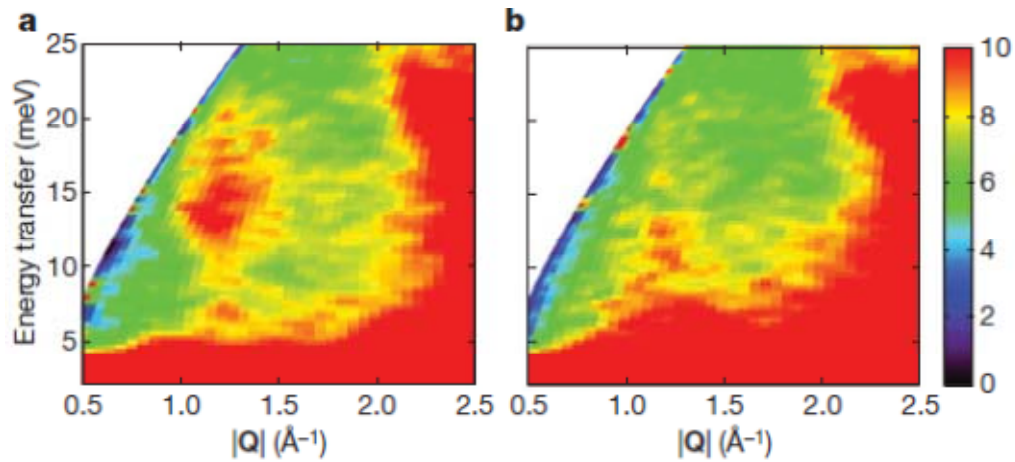


**FIG.6.** Schematic picture of the Fermi surface of  $\text{Ba}_{0.6}\text{K}_{0.4}\text{Fe}_2\text{As}_2$  measured by ARPES. The color bars denote the size of the energy gap, and the upper left inset displays the temperature dependence of the gaps on the three Fermi surface sheets. The  $\alpha$  hole like pocket and  $\beta$  hole like sheet are both centered at the Brillouin zone center  $\Gamma$  point while the electron like  $\gamma$  Fermi sheet is centered at the M point.

As shown in Fig 6, we can see there are three Fermi Surfaces in the Brillouin Zone<sup>19</sup>. All of them are nodeless. In addition, the gaps are uniform in momentum space, which may suggest S wave symmetry. It cannot be  $d_{x^2-y^2}$  symmetry.

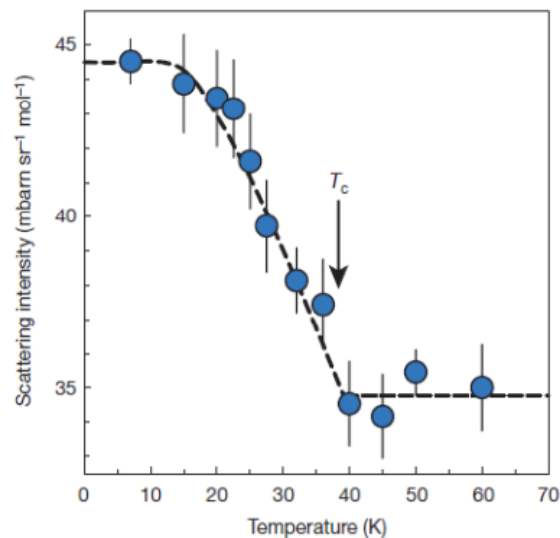
However, it is too early to draw a conclusion now. ARPES can only measure the magnitude of the order parameter  $\Delta(k)$ . It is not phase sensitive. The inelastic neutron scattering can provide us the information about the phase of  $\Delta(k)$ .

Fig 7 shows the inelastic neutron scattering spectrum of  $\text{Ba}_{0.6}\text{K}_{0.4}\text{Fe}_2\text{As}_2$ <sup>20</sup>. The left and right graph corresponds to spectrum taken below ( $T=7\text{K}$ ) and above ( $T=50\text{K}$ ) the superconducting transition temperature respectively. We can see an obvious difference between them. Around  $Q=1.15\text{\AA}^{-1}$  and energy transfer  $\varepsilon=14\text{meV}$ , there is a peak in the spectrum of superconducting state. This peak doesn't show up at 50K. The value of Q characterizing this contribution to the magnetic response corresponds to the periodicity of the antiferromagnetic order within each plane of iron spins observed in the undoped parent compound,  $\text{BaFe}_2\text{As}_2$ .



**Fig.7. Resonant spin excitation in  $\text{Ba}_{0.6}\text{K}_{0.4}\text{Fe}_2\text{As}_2$ .** Inelastic neutron scattering, measured using an incident neutron energy of 60 meV at temperatures below (a, 7 K) and above (b, 50 K)  $T_c$ , shows the development of a magnetic excitation in the superconducting phase at an energy transfer of 14 meV and a momentum transfer of  $1.15 \text{ \AA}^{-1}$ . The strong scattering at low energy transfers arises from the tail of strong elastic nuclear scattering, and the strong increase in scattering at higher values of  $Q$  is due to inelastic phonon scattering.

Fig 8 shows the temperature dependence of this resonant excitation<sup>20</sup>. The intensity is integrated over the region of maximum intensity in Fig 7. We can see an abrupt change around  $T_c$ . In cuprates, there also exists this kind of resonant excitation. As mentioned before, this resonant excitation suggests that  $\Delta_{k+Q} = -\Delta_k$ . In cuprates, it can be explained by the  $d_{x^2-y^2}$  symmetry of  $\Delta(k)$ .



**Fig.8.** Temperature dependence of the resonant spin excitation. The inelastic neutron scattering intensity from  $\text{Ba}_{0.6}\text{K}_{0.4}\text{Fe}_2\text{As}_2$  is integrated over  $Q$  in the range  $1.0\text{--}1.3 \text{ \AA}^{-1}$  and over  $\epsilon$  in the range 12.5–17.5 meV. The error bars are derived from the square root of the raw detector counts. The dashed line is a guide to the eye below  $T_c$  and shows the average value of the integrals above  $T_c$ .

In FeSCs,  $d_{x^2-y^2}$  symmetry is ruled out. If the  $S_{\pm}$  pairing is correct, we can explain this resonant excitation. The holelike Fermi Surface  $\alpha$  has a uniform gap, as well as the electronlike Fermi Surface  $\beta$ . But their gap function  $\Delta(k)$  have different signs.  $Q$  corresponds to the wave vector which connects the Fermi Surface  $\alpha$  and  $\beta$ . Then  $\Delta_{k+Q} = -\Delta_k$ , the resonant excitation can be explained.

To sum, the ARPES measurement and Inelastic neutron scattering experiments support the  $S_{\pm}$  pairing theory.

### 3.4.3 Controversies on pairing mechanism.

Scientists all over the world have done extensive study in Cuprates, but controversies remain. It is the same for the newly discovered iron-based superconductors. There are many controversies. Experiments sometimes contradict with each other.

From above, we conclude that ARPES and Inelastic neutron scattering experiments support the  $S_{\pm}$  pairing theory. But it can't be applied to all iron-based superconductors. The ARPES show that the gaps on all Fermi Surfaces are almost isotropic. However, the penetration-depth experiments in some materials show that they have gap nodes<sup>21</sup>.

An important fact is that many important properties of the Fe-based compounds vary from system to system. The penetration depth measurement on LaFePO indicates that it has nodes<sup>21</sup>, while ARPES measurements show that  $\text{Ba}_{0.6}\text{K}_{0.4}\text{Fe}_2\text{As}_2$  doesn't. Another example is the topology of phase diagram. As we can see in Fig.9, different materials have different phase diagrams<sup>12</sup>.

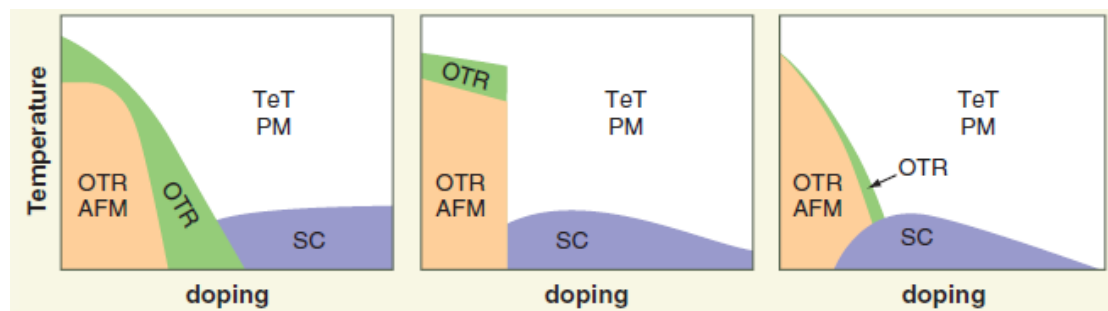


**Fig.9.** Schematic phase diagrams for (A)  $\text{CeFeAsO}_{1-x}\text{F}_x$ ; (B)  $\text{LaFeAsO}_{1-x}\text{F}_x$ ; (C)  $\text{Ba}(\text{Fe}_{1-x}\text{Co}_x)_2\text{As}_2$ . OTR, orthorhombic; TeT, tetragonal crystal structure; AFM, antiferromagnetic; SC, superconducting; PM, paramagnetic phase.

To settle those controversies, maybe we need to do a case-to-case study. Moreover, we should be caution about experiments. Many apparatus have their limits. For example, ARPES is surface sensitive, not bulk sensitive.

## 4. Outlook

There are many problems remaining to be solved in iron-based superconductors. For example, is the  $S_{\pm}$  pairing universal for all iron-based superconductors? What's the attractive force which leads to the formation of Cooper pairs? What is special about iron? Can we achieve higher  $T_c$  in FeSCs?

We look forward to more experiments and theories which can give us clues and answers.

## References

---

- [1] H. K. Onnes, Commun. Phys. Lab. Univ. Leiden **12**, 120 (1911).
- [2] J. Bardeen, L. N. Cooper, J. R. Schrieffer, Phys. Rev. **108**, 1175 (1957).
- [3] Bednorz, J. G., and K. A. Muller, 1986, Z. Phys. B **64**, 189.
- [4] Y. Kamihara, T. Watanabe, M. Hirano, H. Hosono, J. Am. Chem. Soc. **130**, 3296 (2008).
- [5] R. Zhi-An et al., Chin. Phys. Lett. **25**, 2215 (2008).
- [6] Michael R. Norman, Physics **1**, 21 (2008)
- [7] C. C. Tsuei and J. R. Kirtley, Rev. Mod. Phys. **72**, 969 (2000).
- [8] Yang, C. N., 1962, Rev. Mod. Phys. **34**, 694.
- [9] G. R. Stewart, Rev. Mod. Phys. **83**, 1589 (2011).
- [10] Shein, I. R., and A. L. Ivanovskii, 2009a, Solid State Commun. **149**, 1860.
- [11] Deng, Z., X. C. Wang, Q. Q. Liu, S. J. Zhang, Y. X. Lv, J. L. Zhu, R. C. Yu, and C. Q. Jin, 2009, Europhys. Lett. **87**, 37004.
- [12] Fa Wang and Dung-Hai Lee, Science **332**, 200 (2011);
- [13] D. J. Singh, M.-H. Du, Phys. Rev. Lett. **100**, 237003 (2008).
- [14] H. Suhl, B. T. Matthias, L. R. Walker, Phys. Rev. Lett. **3**, 552 (1959).
- [15] I. I. Mazin, D. J. Singh, M. D. Johannes, M. H. Du, Phys. Rev. Lett. **101**, 057003 (2008).
- [16] [http://www-ssrl.slac.stanford.edu/research/highlights\\_archive/high-tc\\_07.html](http://www-ssrl.slac.stanford.edu/research/highlights_archive/high-tc_07.html)
- [17] Chang, J., Eremin, I., Thalmeier, P. & Fulde, Phys. Rev. B **75**, 024503 (2007).
- [18] [http://en.wikipedia.org/wiki/Inelastic\\_neutron\\_scattering](http://en.wikipedia.org/wiki/Inelastic_neutron_scattering)
- [19] Ding, H., et al., 2008, Europhys. Lett. **83**, 47001
- [20] A. D. Christianson, *Nature* **456**, 930-932 (2008)
- [21] J. D. Fletcher et al., Phys. Rev. Lett. **102**, 147001 (2009).